Effect of Coupling on Discontinuous Conduction Mode of Coupled Inductor SIDO Boost Converter

Nupur, *Student Member, IEEE*, and Shabari Nath, *Member, IEEE*

***Abstract*—A single-input dual-output (SIDO) converter with a coupled inductor is a widely used converter to generate two outputs from a single input. The analysis presented in the literature is for continuous conduction mode, where the converters are operating in heavily loaded conditions. While operating, the load may reduce, leading to the discontinuous conduction mode (DCM) of the converter. A coupled inductor SIDO (CI-SIDO) boost converter is analyzed in this article. As this converter combines two boost converters with a common input and a coupled inductor, the DCM operation of one boost affects the other. Due to coupling, it is found that the body diode of the MOSFET turns ON in the DCM operation of the CI-SIDO boost converter. This article finds the conditions to turn ON body diode and its effect on the average values of the inductor current, diode current, and input current. The article also analyzes the CI-SIDO boost when the body diode is not turned ON. This article finds the effect of change in input voltage, load current, and duty ratios on the DCM operation of the CI-SIDO boost. Simulations verify all the obtained conditions in MATLAB/Simulink and experiments using a laboratory prototype. This article is accompanied by a supplementary online document with additional illustrative diagrams and experimental results.**

***Index Terms*—Body diode of MOSFET, coupled inductor, discontinuous conduction mode (DCM), single input dual output (SIDO).**

NOMENCLATURE

L_1, L_2	Coupled inductor windings.
k	Coefficient of coupling.
V_{in}, V_{o1}, V_{o2}	Input, output voltages.
D_1, D_2	Duty ratios of two MOSFETs.
i_{L1}, i_{L2}	Inductor currents.
NN, FF, NF, FN	States of converter where N, F denote ON and OFF states of S_{t1} and S_{t2}, respectively for $i_{L1} > 0, i_{L2} > 0$.
NN_0, FF_0, NF_0, FN_0	States of converter where N, F denote ON and OFF states of S_{t1} and S_{t2}, respectively for $i_{L1} = 0, i_{L2} > 0$.
NN_{bD}, FF_{bD}	States of converter where N, F denote ON and OFF states of S_{t1} and S_{t2}, respectively for $i_{L1} < 0, i_{L2} > 0$.
G_{NNw}, G_{FFw}, G_{NFw}, G_{FNw}, G_{NNw_0}, G_{FFw_0}, G_{NFw_0}, G_{FNw_0}, $G_{NNw_{bD}}$, $G_{FFw_{bD}}$	$\frac{di_w}{dt}$ in states NN, FF, NF, FN, NN_0, FF_0, NF_0, FN_0, NN_{bD}, FF_{bD}, respectively, where $w = 1$ for i_{L1}, $w = 2$ for i_{L2}.
t_{NN}, t_{FF}, t_{NF}, t_{FN}, t_{NN_0}, t_{FF_0}, t_{NF_0}, t_{FN_0} $t_{NN_{bD}}$, $t_{FF_{bD}}$	Duration of states *NN*, *FF*, *NF*, *FN*, NN_0, FF_0, NF_0, FN_0, NN_{bD}, FF_{bD} divided by T_s.
rd_{FN1}, rd_{FN2},	$\frac{V_{\text{in}}}{V_{o1}}$ at which $G_{FN1} = 0$, $G_{FN2} = 0$.
rd_{NF1}, rd_{NF2}	$\frac{V_{\text{in}}}{V_{o2}}$ at which $G_{NF1} = 0$, $G_{NF2} = 0$.

I. INTRODUCTION

THE single-input dual-output (SIDO) converters supply two different outputs from one available input with increased efficiency, power density, and reduced number of components [1]–[4]. The converters have applications in portable electronic devices, fuel cells, electric vehicles, photovoltaic systems, etc. [5]–[7]. In all these applications, the converters are operated in continuous conduction mode (CCM) with heavily loaded conditions [8]–[10]. While operating the SIDO converter in applications like an electric vehicle or photovoltaic system, the converter load may reduce, leading to the discontinuous conduction mode (DCM) of the converter. A complete analysis of the converter is required to efficiently operate the SIDO converters, including the DCM operation.

The inversely coupled inductors are added to the SIDO converters because the dc flux due to one winding cancels the dc flux due to the other windings [2], [3], [8]–[12]. This reduces the flux in the core of the coupled inductor. When operated at a high current, the directly coupled inductors saturate the core more readily than inversely coupled inductors due to reduced flux in the core. Therefore, inversely coupled inductors are a better choice for high-power dc applications. Due to the reduced flux in the core, the volume and weight of the magnetic components reduce. This reduces the overall physical size of SIDO converters.

The literature review on DCM analysis of dc–dc converters is as follows. The literature presents the DCM analysis of converters like a two-phase interleaved boost converter with coupled inductor [12]–[15]. In [12], two CCM and three DCM operating modes are analyzed, including the current, voltage ripples, and

Manuscript received June 24, 2021; revised September 18, 2021; accepted October 2, 2021. Date of publication October 11, 2021; date of current version January 19, 2022. Recommended for publication by Associate Editor W. Huang. *(Corresponding author: Nupur.)*

The authors are with the Department of Electronics and Electrical Engineering, Indian Institute of Technology Guwahati, Guwahati 781039, India (e-mail: nupur.2015@iitg.ac.in; snath@iitg.ac.in).

This article has supplementary material provided by the authors and color versions of one or more figures available at https://doi.org/10.1109/TPEL.2021.3119043.

Digital Object Identifier 10.1109/TPEL.2021.3119043

dc voltage gain analysis of interleaved boost converter with inversely coupled inductors. In [13], more operating modes of interleaved boost converters are added compared to [12]. The DCM and boundary analysis of ten operating modes are discussed with discrete and coupled inductors. However, few operating modes are still ignored. In [14], the dual interleaved buck and boost converters with interphase transformers are analyzed, and major DCM operating regions are presented depending on the voltage ratios and duty cycles. In [15], the complete analysis of interleaved boost converters is presented with all possible operating modes in DCM. The DCM analysis gives rise to many different modes of operation because the forced turn ON of body diodes of the MOSFETs takes place in DCM. Also, the forced conduction of the forward diode takes place due to the presence of coupled inductors.

The literature also presents the solution to parasitic ringing, which happens in all types of dc–dc converters [16], [17]. Due to the parasitic capacitance of MOSFETs and the stray inductor in the circuit, there is a parasitic oscillation in the converters when the inductor currents become zero. The literature also presents the input current ripples analysis for interleaved boost converters in DCM [18] for all possible duty ratios. The coupled inductor interleaved boost converter with single-phase operations for lightly loaded conditions are also discussed in [19]. This phase-shedding is used to improve the efficiency of the converter.

This article focuses on the coupled inductor SIDO (CI-SIDO) boost converter in DCM. The general analysis of the CI-SIDO boost converter in CCM is already published in [7]. Also, the optimum design method of the CI-SIDO boost converter is proposed in [20]. A power electronic converter is usually designed for rated conditions. So, the values of different passive elements (such as L_1 and L_2) are chosen at the design stage according to the rating of the converter. However, the converter may not operate in rated conditions always. The load of the converter may reduce while operating, leading to the DCM of the converter. Therefore, this article evaluates the performance of the CI-SIDO boost converter in DCM.

The CI-SIDO boost converter has two different duty ratios, output voltages, loads, and inductance values. In an interleaved boost converter, the duty ratios of two phases are equal, inductance values are also equal, and the load is common. So, the DCM approach adopted for the interleaved boost converter does not apply to the CI-SIDO boost converter. The number of DCM operating modes of the CI-SIDO boost converter is much more than that of the coupled inductor interleaved boost [15]. The DCM analysis of CI-SIDO boost is compared with the interleaved boost converter in Table I.

The article evaluates the effect of coupling on the DCM analysis of CI-SIDO boost (see Fig. 1). The converter has so many different operating modes due to the coupled inductors, two different duty ratios, and two unequal loads. Furthermore, the turning ON of the body diode due to coupling further adds to the feasible operating modes. Also, the variation of input voltage affects both the boost converters of the CI-SIDO boost converter because of the common input. This article assumes that the first boost converter is in DCM while the second boost is still in CCM to show the effect of the DCM operation of the first boost on the CCM operation of the second boost. However, the approach presented in this article can be extended to CI-SIDO boost when both are in DCM.

TABLE I
CHALLENGES IN DCM ANALYSIS OF CI-SIDO BOOST VERSUS INTERLEAVED BOOST

Basis of comparison	[12], [13], [15]	this paper
Topology	Interleaved Boost	CI-SIDO Boost
Relations between D_1, D_2, L_1, L_2	$D_1 = D_2 = D$, $L_1 = L_2 = L$	$D_1 \neq D_2$, $L_1 \neq L_2$
Output voltage	V_o is common, i.e., only one output	V_{o1}, V_{o2} are different and independent
Slopes of i_{L1}, i_{L2}	Same	Different
Number of DCM waveform patterns for i_{L1} and i_{L2}	10	21*
Forced turning ON of power diodes depend on	k	k, $\frac{L_1}{L_2}$
Turning ON of body diodes depend on	k	k, $\frac{L_1}{L_2}$
Boundaries of DCM operating modes depend on	$\frac{V_{in}}{V_o}$, k	$\frac{V_{in}}{V_{o1}}$, $\frac{V_{in}}{V_{o2}}$, $\frac{L_1}{L_2}$, k
Voltage and current stress	always less than or equal to CCM conditions	may increase or decrease depending on L_1, L_2, k
Duty ratio depends on	V_{in}, V_o, k, i_o	V_{in}, V_{o1}, V_{o2}, k, L_1, L_2, $\frac{L_1}{L_2}$, i_{o1}
Voltage gain depends on	V_{in}, V_o, k, D, i_o	V_{in}, V_{o1}, V_{o2}, k, L_1, L_2, $\frac{L_1}{L_2}$, i_{o1}, D_1, D_2

*Number increases if both boost converters in DCM and gate pulse shift are considered.

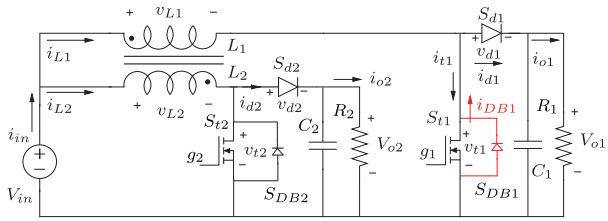

Fig. 1. CI-SIDO boost converter when (a) S_{DB1} is ON and i_{L1} is negative (shown in red color) and (b) S_{DB1} is OFF (shown in black color).

The contributions of the article are as follows.

1) This article presents the effect of coupling on the DCM analysis of a CI-SIDO boost converter. As the CI-SIDO boost converter is a combination of two boost converters, the article presents the effect of DCM operation of the first boost on the second boost when the second boost is at CCM/DCM boundary or in CCM.
2) Due to coupling, the body diodes of MOSFETs turn ON. This article presents the effect of turning ON of the body diode on the DCM operation of the CI-SIDO boost. The conditions to turn ON the body diode are found, and the effect of body diode on the average values of inductor currents, diode currents, and input current is analyzed.
3) The DCM operation of CI-SIDO boost when the body diode is not turned ON is also analyzed. The slopes and average values of inductor, diode, and input currents are also analyzed when the body diode is not turned ON.
4) Different sectors and operating modes of DCM are found by changing input voltage, load current, and duty ratio. This article finds the effect of change in input voltages, load currents, and duty ratios on the DCM operation of the CI-SIDO boost converter.
5) The output voltage gain analysis and the voltage, current stress on semiconductors in DCM are evaluated.

6) Simulations verify the presented analysis in MATLAB/Simulink and experiments by developing a laboratory prototype.

The rest of this article is organized as follows. Section II presents the circuit description of the CI-SIDO boost and the problem formulation. Section III presents the effect of a body diode on DCM operation. Section IV presents the effect of input voltage, load currents, and duty ratios variation in the DCM analysis of the CI-SIDO boost converter. Section V presents the simulation and experimental verifications for different modes of the CI-SIDO boost converter. Finally, Section VI concludes this article.

II. Circuit Description and Problem Formulation

This section presents the circuit description of the CI-SIDO boost converter, which includes the conditions of turning ON of body diodes and the formation of sectors. Then, the problem formulation of this article is presented in detail.

A. Circuit Description of CI-SIDO Boost Converter

The topology of the CI-SIDO boost converter is shown in Fig. 1. The converter has two MOSFETs S_{t1} and S_{t2}, and two diodes S_{d1} and S_{d2}. The converter is the combination of two boost converters with a common input voltage $V_{\rm in}$ and two outputs V_{o1} and V_{o2}. A coupled inductor replaces the individual inductors with a coupling coefficient k, and windings L_1 and L_2. The first inductor current i_{L1} enters DCM, keeping i_{L2} in CCM. The first load current i_{o1} is varied to analyze the DCM operation of CI-SIDO boost, keeping i_{o2} unchanged. Due to the presence of a coupled inductor, the body diode S_{DB1} turns ON when i_{L1} operates in DCM. When S_{DB1} turns ON, negative current flows through it, as shown in Fig. 1 (in red color). When i_{L1} is positive, the current flows through S_{t1}, as shown in Fig. 1 (in black color).

1) Condition to Turn ON Body Diode of MOSFET: The analysis of the CI-SIDO boost converter in Fig. 1 is done to find the condition of turn-ON of S_{DB1}. The voltage across the S_{t1} is given by $v_{t1} = V_{\rm in} - v_{L1}$. When first boost is in DCM, $i_{L1} = 0$. So $v_{L1} = -k\sqrt{\frac{L_1}{L_2}}v_{L2}$ where v_{L2} can take two values, i.e., $V_{\rm in}$ or $V_{\rm in} - V_{o2}$ as second boost is in CCM. Accordingly, v_{t1} is given by

$$v_{t1} = \begin{cases} \left(1 + k\sqrt{\frac{L_1}{L_2}}\right) V_{\rm in} & \text{if } v_{L2} = V_{\rm in} \\ \left(1 + k\sqrt{\frac{L_1}{L_2}}\right) V_{\rm in} - k\sqrt{\frac{L_1}{L_2}} V_{o2} & \text{if } v_{L2} = V_{\rm in} - V_{o2}. \end{cases} \tag{1}$$

To turn ON S_{DB1}, $v_{t1} < 0$. As v_{t1} is always positive when $v_{L2} = V_{\rm in}$, for $v_{t1} < 0$, we obtain the condition as

$$\left(1 + k\sqrt{\frac{L_1}{L_2}}\right) V_{\rm in} - k\sqrt{\frac{L_1}{L_2}} V_{o2} < 0$$

$$\Rightarrow \boxed{\frac{V_{\rm in}}{V_{o2}} < \frac{k\sqrt{\frac{L_1}{L_2}}}{\left(1 + k\sqrt{\frac{L_1}{L_2}}\right)}}. \tag{2}$$

Therefore, it is found that when $v_{L2} = V_{\rm in}$, the body diode is never ON. For $v_{L2} = V_{\rm in} - V_{o2}$, body diode is ON when (2) is satisfied.

2) Formation of Sectors in DCM: The values of slope in each state are presented in Table II. The table presents the following.

1) G_{NN1}, $G_{NN1_{bD}}$, G_{NN2}, G_{NN2_0}, and $G_{NN2_{bD}}$ are always positive as L_1, L_2, k, $V_{\rm in}$, V_{o1}, and V_{o2} are positive.
2) G_{FF1}, G_{FF2}, and G_{FF2_0} are always negative as $V_{\rm in} < V_{o1}$ and $V_{\rm in} < V_{o2}$.
3) G_{FN1}, G_{FN2}, G_{NF1}, and G_{NF2} can take both positive as well as negative values depending on the voltages and coupled inductor parameters.

Using Table II for $G_{FN1} < 0$, we have

$$\frac{\left(1 + k\sqrt{\frac{L_1}{L_2}}\right) V_{\rm in} - V_{o1}}{(1 - k^2) L_1} < 0$$

$$\Rightarrow \boxed{\frac{V_{\rm in}}{V_{o1}} < \frac{1}{\left(1 + k\sqrt{\frac{L_1}{L_2}}\right)} (= rd_{FN1})}. \tag{3}$$

Thus, we find that

$$G_{FN1} \begin{cases} < 0 & \text{for } \frac{V_{\rm in}}{V_{o1}} < rd_{FN1} \\ = 0 & \text{at } \frac{V_{\rm in}}{V_{o1}} = rd_{FN1} \\ > 0 & \text{for } \frac{V_{\rm in}}{V_{o1}} > rd_{FN1}. \end{cases} \tag{4}$$

Similarly, for $G_{FN2} < 0$, we have

$$\frac{\left(1 + k\sqrt{\frac{L_2}{L_1}}\right) V_{\rm in} - k\sqrt{\frac{L_2}{L_1}} V_{o1}}{(1 - k^2) L_2} < 0$$

$$\Rightarrow \boxed{\frac{V_{\rm in}}{V_{o1}} < \frac{k\sqrt{\frac{L_2}{L_1}}}{\left(1 + k\sqrt{\frac{L_2}{L_1}}\right)} (= rd_{FN2})}. \tag{5}$$

Similarly, $\frac{V_{\rm in}}{V_{o2}} < rd_{NF1}$ for $G_{NF1} < 0$ and $\frac{V_{\rm in}}{V_{o2}} < rd_{NF2}$ for $G_{NF2} < 0$, where

$$rd_{NF1} = \frac{k\sqrt{\frac{L_1}{L_2}}}{\left(1 + k\sqrt{\frac{L_1}{L_2}}\right)},\ rd_{NF2} = \frac{1}{\left(1 + k\sqrt{\frac{L_2}{L_1}}\right)}.$$

It is also found that $rd_{NF1} < rd_{NF2}$, the proof of which is as follows:

$$\frac{k\sqrt{\frac{L_1}{L_2}}}{\left(1 + k\sqrt{\frac{L_1}{L_2}}\right)} < \frac{1}{\left(1 + k\sqrt{\frac{L_2}{L_1}}\right)} \Rightarrow 0 < k < 1. \tag{6}$$

Similarly, it can be proved that $rd_{FN2} < rd_{FN1}$. Plotting these values in the $\frac{V_{\rm in}}{V_{o1}}$ versus $\frac{V_{\rm in}}{V_{o2}}$ plane, we obtain the sector diagram shown in Fig. 2 . As shown, nine different sectors are possible for the DCM analysis of the CI-SIDO boost converter. Each sector has a different waveform of inductor currents due to different $\frac{V_{\rm in}}{V_{o1}}$ and $\frac{V_{\rm in}}{V_{o2}}$ ratios. It is also found that the condition to turn ON the body diode in (2) is the same as the conditions of Sectors 1, 2, and 3. Therefore, the body diode is turned ON in these sectors as marked in the sector diagram of Fig. 2.

TABLE II
SLOPES OF INDUCTOR CURRENTS IN FOUR STATES

Inductor current	NN	FF	NF	FN
i_{L1}	$G_{NN1}=\frac{\left(1+k\sqrt{\frac{L_1}{L_2}}\right)V_{in}}{(1-k^2)L_1}$	$G_{FF1}=\frac{\left(1+k\sqrt{\frac{L_1}{L_2}}\right)V_{in}-\left(V_{o1}+k\sqrt{\frac{L_1}{L_2}}V_{o2}\right)}{(1-k^2)L_1}$	$G_{NF1}=\frac{\left(1+k\sqrt{\frac{L_1}{L_2}}\right)V_{in}-k\sqrt{\frac{L_1}{L_2}}V_{o2}}{(1-k^2)L_1}$	$G_{FN1}=\frac{\left(1+k\sqrt{\frac{L_1}{L_2}}\right)V_{in}-V_{o1}}{(1-k^2)L_1}$
i_{L2}	$G_{NN2}=\frac{\left(1+k\sqrt{\frac{L_2}{L_1}}\right)V_{in}}{(1-k^2)L_2}$	$G_{FF2}=\frac{\left(1+k\sqrt{\frac{L_2}{L_1}}\right)V_{in}-\left(V_{o2}+k\sqrt{\frac{L_2}{L_1}}V_{o1}\right)}{(1-k^2)L_2}$	$G_{NF2}=\frac{\left(1+k\sqrt{\frac{L_2}{L_1}}\right)V_{in}-V_{o2}}{(1-k^2)L_2}$	$G_{FN2}=\frac{\left(1+k\sqrt{\frac{L_2}{L_1}}\right)V_{in}-k\sqrt{\frac{L_2}{L_1}}V_{o1}}{(1-k^2)L_2}$
$i_{L1}=0$, i_{L2} CCM, S_{DB1} OFF	$G_{NN2_0}=\frac{V_{in}}{L_2}$	$G_{FF2_0}=\frac{V_{in}-V_{o2}}{L_2}$	$G_{NF2_0}=\frac{V_{in}-V_{o2}}{L_2}$	$G_{FN2_0}=\frac{V_{in}}{L_2}$
i_{L1} negative, i_{L2} CCM, S_{DB1} ON	$G_{NN1_{bD}}=G_{NN1}$ $G_{NN2_{bD}}=G_{NN2}$	$G_{FF1_{bD}}=G_{NF1}$ $G_{FF2_{bD}}=G_{NF2}$	–	–

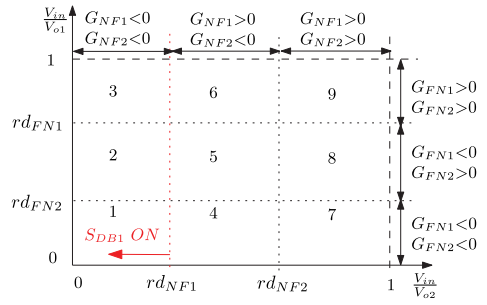

Fig. 2. Sector diagram for DCM analysis of the CI-SIDO boost converter.

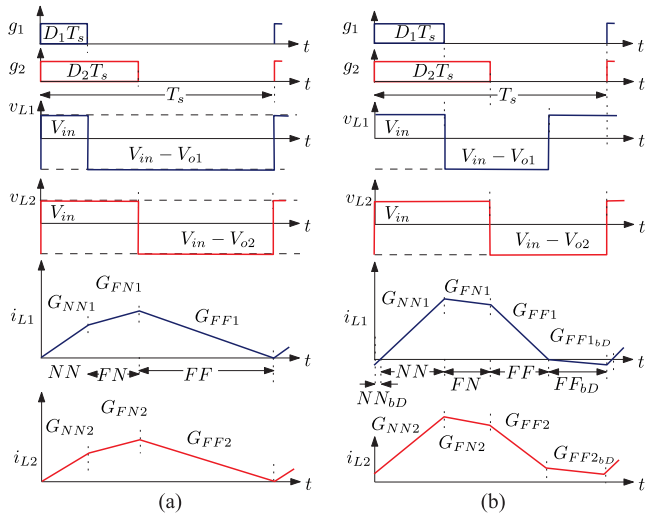

Fig. 3. (a) Both inductor currents i_{L1} and i_{L2} are at boundary for a given load currents. (b) As the first load current decreases, i_{L1} goes to DCM. This shifts i_{L2} to CCM from boundary, without any change in the circuit.

B. Problem Formulation

The waveforms of inductor currents i_{L1} and i_{L2} and voltage across inductors v_{L1} and v_{L2} are shown in Fig. 3. From the figures, we find the following.

1) Both i_{L1} and i_{L2} are at boundary for a given load currents i_{o1} and i_{o2}, as shown in Fig. 3(a).
2) As the load current i_{o1} decreases from the boundary condition, i_{L1} goes to DCM, as shown in Fig. 3(b).
3) As i_{L1} goes to DCM, i_{L2} shifts from boundary to CCM without any change in i_{o2}, as shown in Fig. 3(b).
4) In Fig. 3(b), we observe that i_{L1} is becoming negative.
5) Even if i_{L2} of Fig. 3 is in CCM, its slope changes in state FF_{bD}.

As the load current i_{o1} decreases from the boundary condition to enter DCM, the waveforms of the inductor currents also change. It is also observed that i_{L1} is becoming negative for some portion of the switching period. The change in the input voltage is expected to affect both the boost converters because of the common input voltage. This article aims to find the causes of the above-mentioned behaviors of the CI-SIDO boost converter in detail. All these effects are related to the effect of coupling. Therefore, this article presents a detailed analysis of the CI-SIDO boost converter when the first boost is in DCM while the second boost is still in CCM. This assumption helps in better understanding the effect of coupling on the DCM analysis of the CI-SIDO boost converter.

It is to be noted that the CI-SIDO boost is analyzed with a nonshifted gate pulse, i.e., g_1 and g_2 starts simultaneously. The advantage of the gate pulse shift is in the ripple reduction for CCM operation [7]. In CI-SIDO boost, it is found that the value of shift where inductor current ripples are minimum is not fixed even in CCM [7] unlike interleaved boost converters. As the CI-SIDO boost enters DCM, the inductor current waveform patterns become more complex. So, the process of finding the optimum shift for DCM is again becoming a function of several other parameters. The controller design for this type of shifting is more complex. For any controller, precisely generating this shift is going to be very difficult. Also, during DCM operation, the values of inductor currents become very small. So the amount of ripple is not a concern in DCM. So, to keep it simple, we have chosen to operate the converter for nonshifted gate pulse, i.e., g_1 and g_2 starts simultaneously for DCM.

If the gate pulse of the CI-SIDO boost converter is given a shift, there are conditions when forced turn ON of the power diode takes place. When $v_{L2}=V_{\rm in}-V_{o2}$, S_{d1} is not turned ON forcefully. For $v_{L2}=V_{\rm in}$, the forced turn ON of S_{d1} takes place if the following condition is satisfied:

$$\frac{V_{\rm in}}{V_{o1}}>\frac{1}{(1+k\sqrt{\frac{L_1}{L_2}})}. \tag{7}$$

III. Effect of Body Diode on DCM Operation of CI-SIDO Boost Converter

This section presents the effect of the body diode on the DCM operation of the converter.

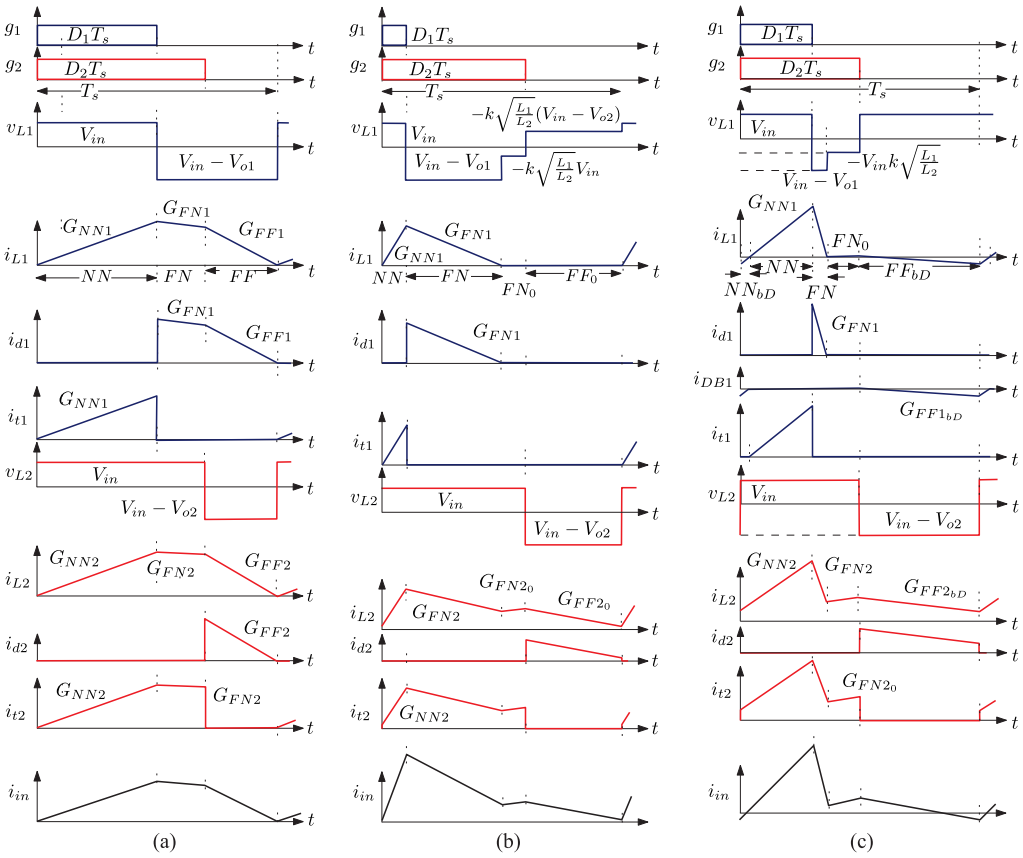

Fig. 4. Theoretical waveforms of g_1, g_2, v_{L1}, i_{L1}, i_{d1}, i_{t1}, v_{L2}, i_{L2}, i_{d2}, i_{t2}, and i_{in} for a constant V_{o1} and V_{o2} at (a) CCM/DCM boundary (b) when S_{DB1} is OFF and (c) when S_{DB1} is ON.

A. DCM Operation When Body Diode Is Turned ON

When body diode, S_{DB1} is turned ON, the currents i_{L1}, i_{d1}, and i_{in} become negative for some values of i_{o1}. This section analyzes the effect of negative currents on the slopes and average values of i_{L1}, i_{L2}, i_{d1}, i_{d2}, and i_{in}, denoted by their corresponding capital letters.

1) Effect on Slopes of i_{L1}, i_{L2}, i_{d1}, i_{d2}, and i_{in} When Body Diode Is Turned ON: When the condition of turning ON of the body diode in (2) is satisfied, the body diode turns ON. The effect of negative currents on the slopes of i_{L1}, i_{L2}, i_{d1}, and i_{d2} are explained using the waveforms shown in Fig. 4(c). As discussed in Section II-A1, the body diode is turned ON when $v_{L2} = V_{\text{in}} - V_{o2}$. Therefore, for the duration of FN_o, $i_{L1} = 0$ and the slopes of i_{L2} changes. The voltages across the inductor windings in FN_o is given as

$$v_{L1} = -k\sqrt{\frac{L_1}{L_2}}v_{L2},\ v_{L2} = (1-k^2)L_2\frac{di_{L2}}{dt} - k\sqrt{\frac{L_2}{L_1}}v_{L1}. \tag{8}$$

Substituting the expression of v_{L1} in v_{L2}, the expression reduces to

$$v_{L2} = L_2\frac{di_{L2}}{dt}. \tag{9}$$

Therefore, for state FN_o where $v_{L2} = V_{\text{in}}$, the slope of i_{L2} called G_{FN2_0} is given by

$$G_{FN2_o} = \frac{V_{\text{in}}}{L_2}. \tag{10}$$

After the duration FN_o, S_{DB1} turns ON and i_{DB1} starts flowing in the negative direction. This duration is called FF_{bD}. Even though S_{DB1} conducts in this state, $G_{FF1_{bD}} = G_{NF1}$ and $G_{FF2_{bD}} = G_{NF2}$, as presented in Table II.

As the slopes of i_{L1} and i_{L2} change, the waveforms of i_{d1}, i_{d2}, and i_{in} change, as shown in Fig. 4(c). As the current i_{DB1} becomes negative up to T_s with negative slope $G_{FF1_{bD}}$, it remains in the negative direction at the stating of the next switching cycle with a positive slope of $G_{NN1_{bD}}$ for NN_{bD}. If the duration of NN_{bD} is smaller than D_1T_s, S_{t1} turns ON with positive i_{L1}. The currents i_{L1} and i_{L2} increase with their respective positive slopes G_{NN1}, G_{NN2} up to D_1T_s. After that i_{L1} and i_{L2} decrease with their respective negative slopes G_{FN1} and G_{FN2}. Thus, in this way, the cycle repeats.

The slopes of input current in the CI-SIDO boost converter is the sum of slopes of the inductor currents in the corresponding state. At boundary in Fig. 4(a), i_{in} starts from 0 as i_{L1} and i_{L2} starts from 0. When S_{DB1} is ON in Fig. 1, i_{in} starts from a negative value as the sum of i_{L1} and i_{L2} at $t = 0$ is negative. As a result, i_{in} becomes negative for some portion of T_s when S_{DB1} is ON.

2) Effect on Average Values of i_{L1}, i_{L2}, i_{d1}, i_{d2}, $i_{\rm in}$ When Body Diode Is Turned ON: To show the effect of turning ON of the body diode on the average values of i_{L1}, i_{L2}, i_{d1}, and i_{d2}, one set of waveform is shown in Fig. 4(a) and (c), where V_{o1} and V_{o2} are kept the same and $V_{\rm in}$ is changed such that body diode S_{DB1} turns ON and negative current flows through it. The average values are compared with the condition when both i_{L1} and i_{L2} are at boundary, as in Fig. 4(a). As the voltages V_{o1} and V_{o2} are to be maintained constant, the duty ratios D_1 and D_2 change in response to the change in input voltage $V_{\rm in}$. For a given $V_{\rm in}$, the first boost converter enters from CCM/DCM boundary to DCM by reducing the load current, i_{o1}. As the average value of i_{d1} is the load current i_{o1}, therefore, the average value of i_{d1} is decreasing as the converter enters from boundary to DCM. The average values of i_{L1}, i.e., I_{L1} decreases as the load current i_{o1} decreases from the boundary value. This is evident from the waveforms of i_{L1} from Fig. 4(c) and (a).

As the second boost is not changed while the first enters from boundary to DCM, the load current of i_{o2} remains the same. Consequently, the average value of i_{d2} does not change. The average values of i_{L2}, i.e., I_{L2} remain approximately the same as the load current of the second boost, i.e., i_{o2} is not changed. The average value of $i_{\rm in}$ can become negative if the sum of average values of i_{L1} and i_{L2} are negative.

B. DCM Operation When Body Diode Is Not Turned ON

When i_{L1} is in DCM, but body diode S_{BD1} is not turned ON, the CI-SIDO boost converter operates in DCM without any negative current. This section analyzes the effect of $i_{L1}=0$ on the slopes and average values of i_{L1}, i_{L2}, i_{d1}, i_{d2}, and $i_{\rm in}$.

1) Effect on Slopes of i_{L1}, i_{L2}, i_{d1}, i_{d2}, and $i_{\rm in}$ When Body Diode Is Not Turned ON: The waveforms are shown in Fig. 4(b). The inductor currents i_{L1} and i_{L2} starts from 0 with their respective slopes G_{NN1} and G_{NN2} in the state NN. After this state, S_{t1} turns OFF and i_{L1} and i_{L2} decrease with slopes G_{FN1} and G_{FN2} in the FN state. However, i_{L1} becomes 0 before turning OFF of S_{t2}. So, this state where S_{t1} is OFF, $i_{L1}=0$, and S_{t2} is ON, is called the FN_0 state. The slopes of i_{L2} in this state are given by G_{FN2_o}, as presented in Table II. The next state is FF_0 where both S_{t1} and S_{t2} are OFF and $i_{L1}=0$. Using (9) in FN_0 and FF_0, the slopes of i_{L2} are given by

$$G_{FN2_o}=\frac{V_{\rm in}}{L_2},\ G_{FF2_o}=\frac{V_{\rm in}-V_{o2}}{L_2}. \tag{11}$$

When S_{DB1} is OFF in Fig. 4(b), $i_{\rm in}$ starts from a positive value as the sum of i_{L1} and i_{L2} at $t=0$ is positive. Therefore, the sum of i_{L1} and i_{L2} are never negative, resulting in a positive $i_{\rm in}$.

2) Effect on Average Values of i_{L1}, i_{L2}, i_{d1}, i_{d2}, and $i_{\rm in}$ When Body Diode Is Not Turned ON: Similar to Section III-A2, the average values of i_{L1}, i_{L2}, i_{d1}, and i_{d2} when S_{DB1} is OFF [see Fig. 4(b)] are compared to its boundary case [see Fig. 4(a)]. The comparisons show that the average values of i_{d1} and i_{L1} decrease as i_{o1} is decreased. This is clearly shown in Fig. 4(b) where the base as well as the height of i_{d1} graph decreases compared to i_{d1} at boundary in Fig. 4(a). The average values of i_{d2} remain same as i_{o2} is not changing. As a result, the variation in average values of i_{L2} is insignificant compared to the average values of i_{L1}. In this case, the average values of i_{L1} are never negative. As the average value of $i_{\rm in}$ is the sum of average values of i_{L1} and i_{L2}; therefore, it is never negative.

IV. Effect of Change in $V_{\rm in}$, i_{o1}, and D_1–Different Modes of CI-SIDO Boost Converter in DCM

In the CI-SIDO boost converters, the output voltages V_{o1} and V_{o2} are to be maintained based on the applications. If $V_{\rm in}$ changes, the values of $\frac{V_{\rm in}}{V_{o1}}$ and $\frac{V_{\rm in}}{V_{o2}}$ change. This changes the sector of operation of the CI-SIDO boost converter, as shown in Fig. 2. The change in sector changes the waveforms of i_{L1} and i_{L2}, which is actually affecting the DCM operation of the CI-SIDO boost converter. Therefore, each sector is analyzed, and the ranges of $V_{\rm in}$, i_{o1}, and D_1 are calculated for each sector. The formation of different modes is also discussed, followed by the grouping of sectors based on a similar i_{L1} pattern. The voltage and current stress on semiconductors are analyzed, followed by the analysis of the output voltage gain.

A. Formation of Modes and Grouping of Sectors Based on Similar i_{L1} Patterns

As discussed earlier, the inductor current waveforms of all nine sectors are different from each other. For a given V_{o1}, V_{o2}, the range of $V_{\rm in}$ for each sector is calculated using Fig. 2. For example, the range of $V_{\rm in}$ for Sector 1 is

$$\begin{aligned} &0<V_{\rm in}<V_{o2}.rd_{NF1},\ 0<V_{\rm in}<V_{o1}.rd_{FN2}\\ &\Rightarrow 0<V_{\rm in}<\min(V_{o1}.rd_{FN2},V_{o2}.rd_{NF1}). \end{aligned} \tag{12}$$

Similarly, the range of $V_{\rm in}$ for all other sectors is calculated and presented in Table III.

Within a sector, the inductor current patterns further change depending on the load currents and duty ratios. Therefore, modes are formed within the sector. Sectors 1, 2, 4, 5, 7, and 8 are divided into three modes whereas Sectors 3, 6, and 9 have only one mode. For example, the physical meaning of Sector "1" Mode "1a" is that its inductor current slope conditions are $G_{NN1}>0$, $G_{NF1}<0$, $G_{FN1}<0$, $G_{FF1}<0$, $G_{NN2}>0$, $G_{NF2}<0$, $G_{FN2}<0$, and $G_{FF2}<0$, the load range is $i_{o11b}<i_{o1}<i_{o1bd}$, and the range of duty ratio is $D_{1_{1b}}<D_1<t_{NN}$.

This article analyzes CI-SIDO boost with i_{L1} in DCM, keeping i_{L2} in CCM. Due to this considered assumption, the sectors of the CI-SIDO boost converter are divided into four groups based on the similar patterns of i_{L1}. The analysis of one waveform from each group is sufficient to show the behavior of i_{L1} for each group.

The durations of states of each inductor current waveform pattern are discussed here. For a given value of coupled inductors, output, and input voltages, the slopes of the CI-SIDO boost converter are known. For the required t_{FF}, the waveform of i_{L1} from Mode 1a of Fig. 5(a) gives

$$t_{NN_{bD}}=\frac{|G_{NF1}|(1-D_2-t_{FF})}{G_{NN1}}$$

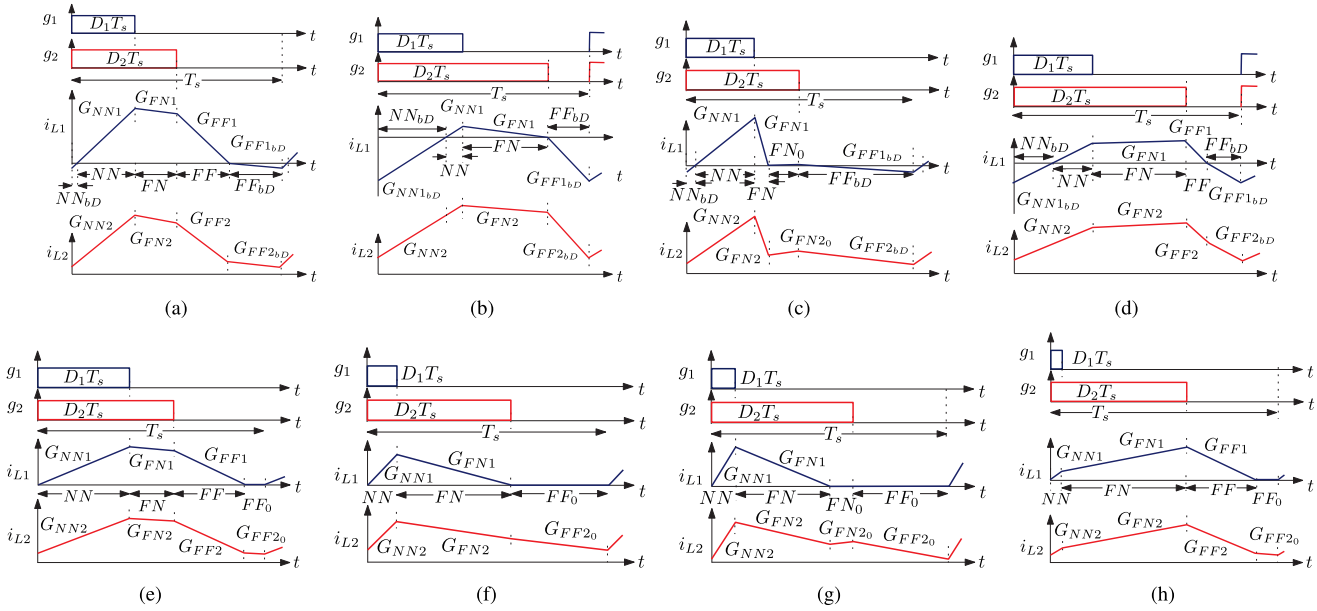

Fig. 5. Theoretical waveforms of g_1, g_2, i_{L1}, and i_{L2} when operating in modes (a) 1a, (b) 1b, (c) 1c, (d) 3, (e) 4a, (f) 4b, (g) 4c, and (h) 6.

TABLE III
RANGE OF INPUT VOLTAGE IN DIFFERENT MODES OF DCM IN CI-SIDO BOOST CONVERTER

Sector	Modes	Range of V_{in}
1	1a 1b 1c	$0 < V_{in} < \min(V_{o1}rd_{FN2}, V_{o2}rd_{NF1})$
2	2a 2b 2c	$\max(V_{o1}.rd_{FN2}, 0) < V_{in} < \min(V_{o1}.rd_{FN1}, V_{o2}.rd_{NF1})$
3	3	$\max(V_{o1}.rd_{FN1}, 0) < V_{in} < \min(V_{o1}, V_{o2}.rd_{NF1})$
4	4a 4b 4c	$\max(V_{o2}.rd_{NF1}, 0). < V_{in} < \min(V_{o1}.rd_{FN2}, V_{o2}.rd_{NF2})$
5	5a 5b 5c	$\max(V_{o1}.rd_{FN2}, V_{o2}.rd_{NF1}) < V_{in} < \min(V_{o1}.rd_{FN1}, V_{o2}.rd_{NF2})$
6	6	$\max(V_{o1}rd_{FN1}, V_{o2}rd_{NF1}) < V_{in} < \min(V_{o1}, V_{o2}rd_{NF2})$
7	7a 7b 7c	$\max(0, V_{o2}.rd_{NF2}) < V_{in} < \min(V_{o1}.rd_{FN2}, V_{o2})$
8	8a 8b 8c	$\max(V_{o1}.rd_{FN2}, V_{o2}.rd_{NF2}) < V_{in} < \min(V_{o1}.rd_{FN1}, V_{o2})$
9	9	$\max(V_{o1}rd_{FN1}, V_{o2}rd_{NF2}) < V_{in} < \min(V_{o1}, V_{o2})$

$$t_{FN} = \frac{\left(D_2 - t_{NN_{bD}} - t_{FF}\frac{|G_{FF1}|}{|G_{NN1}|}\right)}{(1 + \frac{|G_{FN1}|}{|G_{NN1}|})}$$

$$t_{NN} = t_{FN}\frac{|G_{FN1}|}{|G_{NN1}|} + t_{FF}\frac{|G_{FF1}|}{|G_{NN1}|}$$

$$D_1 = t_{NN_{bD}} + t_{NN}$$

$$i_{o1} = \frac{T_s}{2}[t_{FF}(t_{FF} + t_{FN})|G_{FF1}| + t_{NN}t_{FN}G_{NN1}]. \tag{13}$$

Now, at CCM/DCM boundary, we have $t_{NN_{bD}} = t_{FF_{bD}} = 0$, $t_{FF} = (1 - D_2)$, and $D_2 = t_{NN} + t_{FN}$. The obtained values of $i_{o1} = i_{o1bd}$ and $D_1 = t_{NN}$ at the CCM/DCM boundary are

$$\frac{T_s}{2}[t_{NN}(D_2 - t_{NN})G_{NN1} + (1 - D_2)(1 - t_{NN})|G_{FF1}|]$$

$$\text{where } t_{NN} = \frac{D_2|G_{FN1}| + (1 - D_2)|G_{FF1}|}{G_{NN1} + G_{FN1}}. \tag{14}$$

Therefore, i_{L1} remains in DCM when $i_{o1} < i_{o1bd}$ and $D_1 < t_{NN}$, as presented in Table III. Now, the details of Mode 1b are obtained using Fig. 5(b) as follows:

$$t_{NN_{bD}} = \frac{G_{NF1}(1 - D_2)}{G_{NN1}},\ t_{NN} = \frac{(D_2 - t_{NN_{bD}})}{(1 + \frac{G_{NN1}}{|G_{FN1}|})}$$

$$t_{FN} = \frac{G_{NN1}}{|G_{FN1}|}\frac{(D_2 - t_{NN_{bD}})}{\left(1 + \frac{G_{NN1}}{|G_{FN1}|}\right)},\ D_1 = t_{NN_{bD}} + t_{NN}$$

$$i_{o1} = \frac{T_s}{2}t_{FN}^2|G_{FN1}|. \tag{15}$$

Finding the values of $i_{o1} = i_{o11b}$ and $D_1 = D_{1_{1b}}$ at Mode 1b, we obtain

$$i_{o11b} = \frac{|G_{FN1}|(D_2T_sG_{NN1} - |G_{NF1}|(1 - D_2)T_s)^2}{2T_s(|G_{FN1}| + G_{NN1})^2}$$

$$D_{1_{1b}} = \frac{D_2G_{FN1} + (1 - D_2)G_{NF1}}{G_{NN1} + G_{FN1}}. \tag{16}$$

Therefore, i_{L1} remains in Mode 1a when $i_{o11b} < i_{o1} < i_{o1bd}$ and $D_{1_{1b}} < D_1 < t_{NN}$. At $i_{o1} = i_{o11b}$ and $D_1 = D_{1_{1b}}$, the converter is at Mode 1b. After that if $i_{o1} < i_{o11b}$ and $D_1 < D_{1_{1b}}$,

TABLE IV
DURATION OF STATES, OUTPUT VOLTAGE GAIN, AND VOLTAGE STRESS ON SEMICONDUCTORS OF CI-SIDO BOOST CONVERTER IN DCM

Similar Modes	Duration of states	Input-output relations	$v_{t1\,max} = \max\{\}$	$v_{d1\,max} = \min\{\}$
1b, 2b	$t_{FF_{bD}} = (1 - D_2)$, $t_{NN_{bD}} = \frac{G_{NF1}(1-D_2)}{G_{NN1}}$, $t_{NN} = \frac{(D_2 - t_{NN_{bD}} - t_{FN_0})}{(1+\frac{G_{NN1}}{\lvert G_{FN1}\rvert})}$, $t_{FN} = \frac{G_{NN1}}{\lvert G_{FN1}\rvert}\frac{(D_2 - t_{NN_{bD}} - t_{FN_0})}{(1+\frac{G_{NN1}}{\lvert G_{FN1}\rvert})}$	$\frac{V_{o1}}{V_{in}} = \frac{1}{(D_2 - D_1)}$	V_{o1}	$-V_{o1}$
1c, 2c	$t_{FF_{bD}} = (1 - D_2)$, $t_{NN_{bD}} = \frac{G_{NF1}(1-D_2)}{G_{NN1}}$, $t_{NN} = \frac{(D_2 - t_{NN_{bD}} - t_{FN_0})}{(1+\frac{G_{NN1}}{\lvert G_{FN1}\rvert})}$, $t_{FN} = \frac{G_{NN1}}{\lvert G_{FN1}\rvert}\frac{(D_2 - t_{NN_{bD}} - t_{FN_0})}{(1+\frac{G_{NN1}}{\lvert G_{FN1}\rvert})}$	$\frac{V_{o1}}{V_{in}} = \frac{1 - t_{FN_0} q_2}{t_{FN}}$	$\{V_{o1}, q_2 V_{in}\}$	$\{-V_{o1}, q_2 V_{in} - V_{o1}\}$
3	$t_{NN_{bD}} = \frac{\lvert G_{NF1}\rvert(1 - D_2 - t_{FF})}{G_{NN1}}$, $t_{FN} = \frac{(D_2 - t_{NN_{bD}} - t_{FF}\frac{\lvert G_{FF1}\rvert}{\lvert G_{NN1}\rvert})}{(1 - \frac{\lvert G_{FN1}\rvert}{\lvert G_{NN1}\rvert})}$, $t_{NN} = t_{FF}\frac{\lvert G_{FF1}\rvert}{\lvert G_{NN1}\rvert} - t_{FN}\frac{\lvert G_{FN1}\rvert}{\lvert G_{NN1}\rvert}$	$\frac{V_{o1}}{V_{in}} = \frac{1}{(t_{FN} + t_{FF})}$	V_{o1}	$-V_{o1}$
4a, 5a, 7a, 8a	$t_{NN} = \frac{G_{FN1} D_2 + \lvert G_{FF1}\rvert t_{FF}}{(G_{NN1} + G_{FN1})}$, $t_{FN} = D_2 - t_{NN}$	$\frac{V_{o1}}{V_{in}} = \frac{1 - t_{FF_0} q_2}{(t_{FF} + t_{FN})} + \frac{q_1 t_{FF_0}}{(t_{FF} + t_{FN})}\frac{V_{o2}}{V_{in}}$	$\left\{ \begin{array}{l} V_{o1}, \\ q_2 V_{in} - q_1 V_{o2} \end{array} \right\}$	$\left\{ \begin{array}{l} -V_{o1}, q_2 V_{in} \\ -V_{o1} - q_1 V_{o2} \end{array} \right\}$
4b, 5b, 7b, 8b	$t_{FF} = (1 - D_2), t_{FN}\{1 + \frac{G_{FN1}}{G_{NN1}}\} = D_2$, $t_{NN} = \frac{G_{FN1} t_{FN}}{G_{NN1}}$	$\frac{V_{o1}}{V_{in}} = \frac{D_2 q_2 - q_1}{(D_2 - D_1)} + \frac{k\sqrt{\frac{L_1}{L_2}}(1 - D_2)}{(D_2 - D_1)}\frac{V_{o2}}{V_{in}}$	$\left\{ \begin{array}{l} V_{o1}, \\ q_2 V_{in} - q_1 V_{o2} \end{array} \right\}$	$\left\{ \begin{array}{l} -V_{o1}, q_2 V_{in} \\ -V_{o1} - q_1 V_{o2} \end{array} \right\}$
4c, 5c, 7c, 8c	$t_{FF_0} = (1 - D_2)$, $t_{NN} = \frac{G_{FN1} t_{FN}}{G_{NN1}}$, $t_{FN}\{1 + \frac{G_{FN1}}{G_{NN1}}\} = D_2 - t_{FN_0}$	$\frac{V_{o1}}{V_{in}} = \frac{D_1 + t_{FN} - q_1(t_{FN_0} + t_{FF_0})}{t_{FN}} + \frac{k\sqrt{\frac{L_1}{L_2}} t_{FF_0}}{t_{FN}}\frac{V_{o2}}{V_{in}}$	$\left\{ \begin{array}{l} q_2 V_{in} - q_1 V_{o2}, \\ q_2 V_{in}, V_{o1} \end{array} \right\}$	$\left\{ \begin{array}{l} q_2 V_{in} - V_{o1} - q_1 V_{o2}, \\ q_2 V_{in} - V_{o1}, -V_{o1} \end{array} \right\}$
6, 9	$t_{NN} = \frac{\lvert G_{FF1}\rvert t_{FF} - G_{FN1} D_2}{(G_{NN1} - G_{FN1})}$, $t_{FN} = D_2 - t_{NN}$	$\frac{V_{o1}}{V_{in}} = \frac{1 - t_{FF_0} q_2}{(t_{FF} + t_{FN})} + \frac{q_1 t_{FF_0}}{(t_{FF} + t_{FN})}\frac{V_{o2}}{V_{in}}$	$\left\{ \begin{array}{l} V_{o1}, \\ q_2 V_{in} - q_1 V_{o2} \end{array} \right\}$	$\left\{ \begin{array}{l} -V_{o1}, q_2 V_{in} \\ -V_{o1} - q_1 V_{o2} \end{array} \right\}$
$q_1 = k\sqrt{\frac{L_1}{L_2}}$, $q_2 = (1 + k\sqrt{\frac{L_1}{L_2}})$				

the converter operates in Mode 1c. As this article assumes that only i_{L1} is in DCM, the ranges of i_{o1} and D_1 are also valid for modes of Sector 2, i.e., Modes 2a, 2b, and 2c. Similarly, the ranges of V_{in}, i_{o1}, and D_1 for all the sectors and modes are presented in Table V.

The analysis of other sectors show that Sector 3 has only one pattern, as shown in Fig. 5(d). Also, from Fig. 2 and Table V, we find that Sectors 6 and 9 have same waveform of i_{L1} with only one waveform pattern, as shown in Fig. 5(h). Similarly, out of Sectors 4, 5, 7, and 8, the waveform of Sector 4 is shown in Fig. 5(e)–(g), which has three operating modes. The value of i_{o1} corresponding to Mode 4b is given by

$$i_{o1\,4b} = \frac{|G_{FN1}| G_{NN1}^2 D_2^2 T_s}{2(G_{NN1} + |G_{FN1}|)^2}. \tag{17}$$

Therefore, this section shows that the CI-SIDO boost converter has nine sectors, which are grouped into four groups based on similar i_{L1} patterns. Also, Sectors 1, 2, 4, 5, 7, and 8 are further divided into three modes. The waveforms from each mode and group are presented in Fig. 5. For each waveform, the durations of states are presented in Table IV.

The summary of the sectors, modes, and the group of sectors are presented in Table V. The sectors are a group of similar inductor current waveforms based on the inductor current slope conditions. Within the sectors, the inductor current patterns are further changing with load currents and duty ratios. For

TABLE V
DIFFERENT SECTORS AND MODES IN CI-SIDO BOOST CONVERTER WHEN i_{L1} IS IN DCM WHILE i_{L2} IS IN CCM

Sector	Modes	Slopes of i_{L1}	Range of i_{o1}	Range of D_1	sequence of states	Slopes of i_{L2}
1	1a	S-III	C-I	D-I	A-I	S-III
2	2a					S-II
1	1b		C-II	D-II	A-II	S-III
2	2b					S-II
1	1c		C-III	D-III	A-III	S-III
2	2c					S-II
3	3	S-II	C-III	D-III	A-I	S-II
4	4a	S-I	C-IV	D-IV	A-IV	S-III
5	5a					S-II
7	7a					S-I
8	8a					S-IV
4	4b		C-V	D-V	A-V	S-III
5	5b					S-II
7	7b					S-I
8	8b					S-IV
4	4c		C-VI	D-VI	A-VI	S-III
5	5c					S-II
7	7c					S-I
8	8c					S-IV
6	6	S-IV	C-I	D-I	A-IV	S-II
9	9					S-IV

S-I: $G_{NFw} > 0$, $G_{FNw} < 0$; S-II: $G_{NFw} < 0$, $G_{FNw} > 0$
S-III: $G_{NFw} < 0$, $G_{FNw} < 0$; S-IV: $G_{NFw} > 0$, $G_{FNw} > 0$
C-I: $i_{o11b} < i_{o1} < i_{o1bd}$; D-I: $D_{1_{1b}} < D_1 < t_{NN}$
C-III: $0 < i_{o1} < i_{o11b}$; D-III: $0 < D_1 < D_{1_{1b}}$
C-IV: $i_{o14b} < i_{o1} < i_{o1bd}$; D-IV: $D_{1_{4b}} < D_1 < t_{NN}$
C-II: $= i_{o1bd}$; D-II: $= D_{1_{1b}}$, C-V: $= i_{o14b}$; D-V: $= D_{1_{4b}}$
C-VI: $0 < i_{o1} < i_{o14b}$; D-VI: $0 < D_1 < D_{1_{4b}}$
A-I: $NN_{bD} \rightarrow NN \rightarrow FN \rightarrow FF \rightarrow FF_{bD}$
A-II: $NN_{bD} \rightarrow NN \rightarrow FN \rightarrow FF_{bD}$
A-III: $NN_{bD} \rightarrow NN \rightarrow FN \rightarrow FN_0 \rightarrow FF_{bD}$
A-IV: $NN \rightarrow FN \rightarrow FF \rightarrow FF_0$
A-V: $NN \rightarrow FN \rightarrow FF_0$, A-VI: $NN \rightarrow FN \rightarrow FN_0 \rightarrow FF_0$
$D_{1_{bd}} = \frac{(1-D_2)G_{FF1} - D_2 G_{FN1}}{G_{NN1} - G_{FN1}}$, $D_{1_{4b}} = \frac{D_2 G_{FN1}}{G_{NN1} + G_{FN1}}$
$D_{1_{1b}} = \frac{D_2 G_{FN1} + (1-D_2) G_{NF1}}{G_{NN1} + G_{FN1}}$

one inductor current slope condition, one particular type of waveforms pattern represents one mode. From Table V, it is clear that four groups of sectors are possible based on the similar inductor current pattern.

B. Voltage and Current Stress on Semiconductors

As the load currents in DCM are very small compared to CCM, the peak values of MOSFETs and diodes are less compared to CCM. Therefore, the current stress on the MOSFETs and diodes is less compared to CCM. The peak values of MOSFET current for all the modes are

$$i_{t1\max} = G_{NN1} t_{NN} T_s. \tag{18}$$

The peak values of diode current are given by

$$i_{d1\max} = \begin{cases} G_{NN1} t_{NN} T_s + G_{FN1} t_{FN} T_s & \text{for Sectors 3, 6, 9} \\ G_{NN1} t_{NN} T_s & \text{for other sectors.} \end{cases}$$

The maximum current through the body diode is given by

$$i_{DB1\max} = G_{FF1_{bD}} t_{FF_{bD}} T_s. \tag{19}$$

The maximum voltage across the MOSFET and diode depends on the coupled inductor parameters. Compared with their CCM values, the voltage stress may increase or decrease depending on the coupled inductor parameters. The maximum voltage stress on MOSFET and diode is presented in Table IV.

C. Output Voltage Gain Analysis

By applying the volt-second balance for v_{L1} in Mode 1a [see Fig. 5(a)] where the body diode is ON, the input–output voltage relations are calculated as

$$V_{\text{in}}(1 - t_{FN} - t_{FF}) + (V_{\text{in}} - V_{o1})(t_{FN} + t_{FF}) = 0$$
$$\Rightarrow \frac{V_{o1}}{V_{\text{in}}} = \frac{1}{(t_{FN} + t_{FF})}. \tag{20}$$

Now, applying the volt-second balance for v_{L1} in Mode 4b [see Fig. 5(f)] where the body diode is not ON, the input–output voltage relations are calculated as

$$V_{\text{in}} D_1 + (V_{\text{in}} - V_{o1})(D_2 - D_1)$$
$$+ k\sqrt{\frac{L_1}{L_2}}(V_{o2} - V_{\text{in}})(1 - D_2) = 0$$
$$\Rightarrow \frac{V_{o1}}{V_{\text{in}}} = \frac{D_2(1 + k\sqrt{\frac{L_1}{L_2}}) - k\sqrt{\frac{L_1}{L_2}}}{(D_2 - D_1)} + \frac{k\sqrt{\frac{L_1}{L_2}}(1 - D_2)}{(D_2 - D_1)} \frac{V_{o2}}{V_{\text{in}}}. \tag{21}$$

The input–output voltage relations of all the remaining waveforms are presented in Table IV. It is found that the input–output voltage relations in DCM depend on both the output voltages in addition to the coupled inductor values. As i_{L2} is in CCM, the input–output voltage relation is the same as CCM

$$\frac{V_{o2}}{V_{\text{in}}} = \frac{1}{(1 - D_2)}. \tag{22}$$

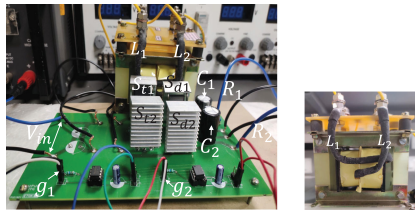

(a) (b)

Fig. 6. Experimental setup. (a) CI-SIDO boost. (b) Coupled inductor.

V. Simulation and Experimental Verifications

A. Simulation Verifications

The CI-SIDO boost converter is simulated in MATLAB/Simulink. The coupled inductor selected is $L_1 = 48.00\,\mu$H, $L_2 = 120.00\,\mu$H, and $k = 0.8$. The converter is operated with a switching frequency of 100 kHz. Suppose, the output voltage to be maintained is $V_{o1} = 10$ V and $V_{o2} = 15$ V. For the given values of L_1, L_2, k, V_{o1}, and V_{o2}, the range of V_{in} is calculated for all the sectors using column 3 of Table III. It is found that the feasible range of V_{in} is obtained for Sectors 1, 4, 5, 8, and 9 only. The respective ranges obtained are $0 < V_{\text{in}} < 5.04$, $5.04 < V_{\text{in}} < 5.58, 5.58 < V_{\text{in}} < 6.62, 6.62 < V_{\text{in}} < 6.64$, and $6.64 < V_{\text{in}} < 10$. Therefore, as V_{in} varies from 0 to 10 V, the sectors of the converter changes.

The waveform of I_{L1} versus i_{o1} is shown in Fig. 7(a). For i_{o1} higher than CCM/DCM boundary, I_{L1} is a straight line passing through the origin with slope $\frac{1}{(1-D_1)}$. As i_{o1} decreases and enters DCM, Mode 1a starts. The converter remains in Mode 1a until i_{o1} is greater than (16). As i_{o1} decreases further below (16), the converter enters Mode 1c. It is found that I_{L1} is negative for some values of i_{o1} due to the turning ON of S_{DB1}. The dotted lines represent the I_{L1} values in CCM. It is found that the value of I_{L1} in DCM has decreased from the boundary values. As the V_{in} is increased, the converter remains in Sector 1; however, I_{L1} is decreased and CCM/DCM boundary is increased. This is shown in Fig. 7(b).

It is to be noted that as V_{in} is changed, D_2 also changes because of the common input voltage V_{in}. However, as V_{o2} and R_2 are not changed. i_{o2} is not changed. Consequently, there is no significant change in I_{L2} as i_{o1} is changed.

The waveform of D_1 versus i_{o1} is shown in Fig. 7(c). The graphs show that as i_{o1} decreases from CCM/DCM boundary, the constant D_1 starts decreasing. As V_{in} is increased, D_1 decreases. As expected, in DCM the duty ratios become load dependent.

Similar simulation graphs are shown for Sector 9 in Fig. 8(a) and (c). The graphs in Fig. 8(b) and (d) show that as V_{in} is changed, the sector of the converter is changed. For $V_{\text{in}} = 5.3$ V, the converter operates in Sector 4, which changes to Sectors 5 and 6 as V_{in} further changes to 6.3 and 6.6 V.

The analysis in all the sectors show that the effect of turning ON of S_{DB1} does not change I_{L1} much. Though it depends on the L_1, L_2, k, D_1, D_2, and V_{in}, the average value I_{L1} becomes negative only in Sector 1 for very small values of i_{o1}.

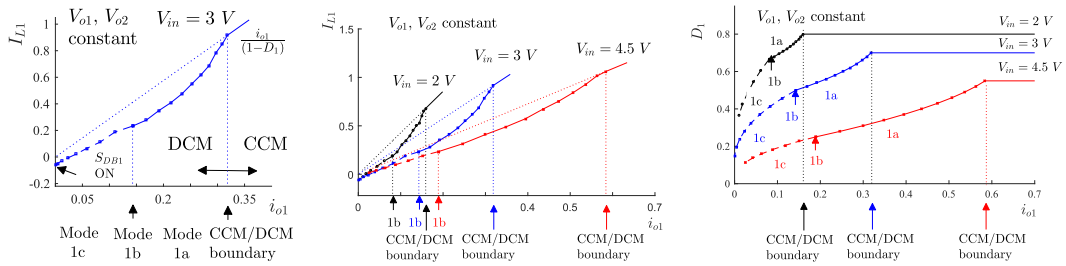

Fig. 7. (a) For a constant output–input voltages, the average value of i_{L1} decreases as i_{o1} is decreased. The negative average value of i_{L1} is due to S_{DB1} ON (Sector 1). (b) Average value of i_{L1} increases as the input voltage is decreased. (c) D_1 decreases as i_{o1} is decreased in DCM.

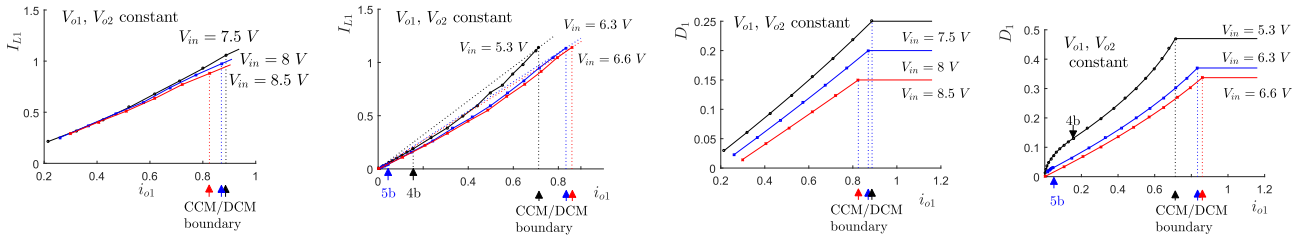

Fig. 8. For a constant output–input voltages, the average value of i_{L1} decreases as i_{o1} is decreased for (a) Sector 9, and (b) Sectors 4, 5, and 8. There is no negative I_{L1} as S_{DB1} is never ON. The average value of i_{L1} increases as input voltage is decreased in both the cases, and D_1 decreases as i_{o1} is decreased in DCM for (c) Sector 9, and (d) Sectors 4, 5, and 8.

B. Experimental Verifications

To verify the sectors and modes presented in this article, a 100-W laboratory prototype of the CI-SIDO boost converter is designed, as shown in Fig. 6. The converter is made using MOSFETs with part number IRFP90N20DPBF and diodes with part number RHRP30120. The input voltage V_{in} given is 4 V, which is taken from a regulated dc supply of 64 V, 20 A. The capacitors of 100 μF are used. The rheostats are used as a load to the CI-SIDO boost converter that is changing for different modes. The currents and voltages are measured using current and differential probes in a four-channel mixed domain oscilloscope. Although the analysis presented in this article is valid for any parameters of a coupled inductor, this article presents the experiments for a ferrite core-coupled inductor with $k = 0.8$, $L_1 = 48\,\mu$H, and $L_2 = 120\,\mu$H. The gate pulses g_1 and g_2 are generated using an FPGA kit numbered NI sbRIO 9637, which is programmed in the LabView platform.

The values of $rd_{FN1}, rd_{FN2}, rd_{NF1}$, and rd_{NF2} are obtained as 0.66, 0.56, 0.34, and 0.44 using (1), respectively. For given $V_{\text{in}} = 4$ V, the ranges of V_{o1} and V_{o2} are obtained for each sector and mode. The values of V_{o1} is varied by changing R_1 and D_1 as the first boost is operated in DCM and V_{o2} is varied by changing D_2 as the second boost is operated in CCM.

For Sector 1, the ranges obtained are $0 < (V_{\text{in}}/V_{o1}) < 0.56$ and $0 < (V_{\text{in}}/V_{o2}) < 0.34$. The example of Mode 1a is shown in Fig. 9(a) for $V_{\text{in}}/V_{o1} = 0.55$ and $V_{\text{in}}/V_{o2} = 0.32$ such that D_1 and D_2 obtained are 0.18 and 0.7, and R_1 and R_2 obtained are 24 and 90 Ω, respectively. The Mode 1b is shown in Fig. 9(b) for $V_{\text{in}}/V_{o1} = 0.55$ and $V_{\text{in}}/V_{o2} = 0.32$ such that D_1 and D_2 obtained are 0.18 and 0.7, and R_1 and R_2 obtained are 50.4 and 90 Ω, respectively. The Mode 1c is shown in Fig. 9(c) for $V_{\text{in}}/V_{o1} = 0.47$ and $V_{\text{in}}/V_{o2} = 0.32$ such that D_1 and D_2 obtained are 0.18 and 0.7, and R_1 and R_2 obtained are 125.8 and 90 Ω, respectively. Likewise, all the other modes are generated in the experiments. The results for Sectors 1, 3, 4, and 6 are shown in Fig. 9. The experimental results for the remaining sectors are presented in supplementary material. As discussed in Section V, we observe that the body diode S_{DB1} is ON in Sectors 1 and 3 only. In all the remaining sectors, there is no turning ON of the body diode S_{DB1}. The ringing in the experimental results is due to the parasitic inductances and capacitances present in the circuit.

C. Findings

The following are the findings of the analysis, simulation, and experiment of CI-SIDO boost converter.

1) *Effect of DCM operation of the first boost on the second when second boost is at boundary or CCM:* As the first boost enters DCM, the slopes of i_{L1} and i_{L2} change in each state. This changes the waveforms of i_{L1}, i_{L2}, i_{d1}, i_{d2}, and i_{in}. The calculated slopes are presented in Table II.
2) *Conditions to turn* ON *body diode:* When the first boost is in DCM and the second boost in CCM, it is found that the body diode turns ON in Sectors 1, 2, and 3 only. The condition to turn ON S_{DB1} is given by (2).

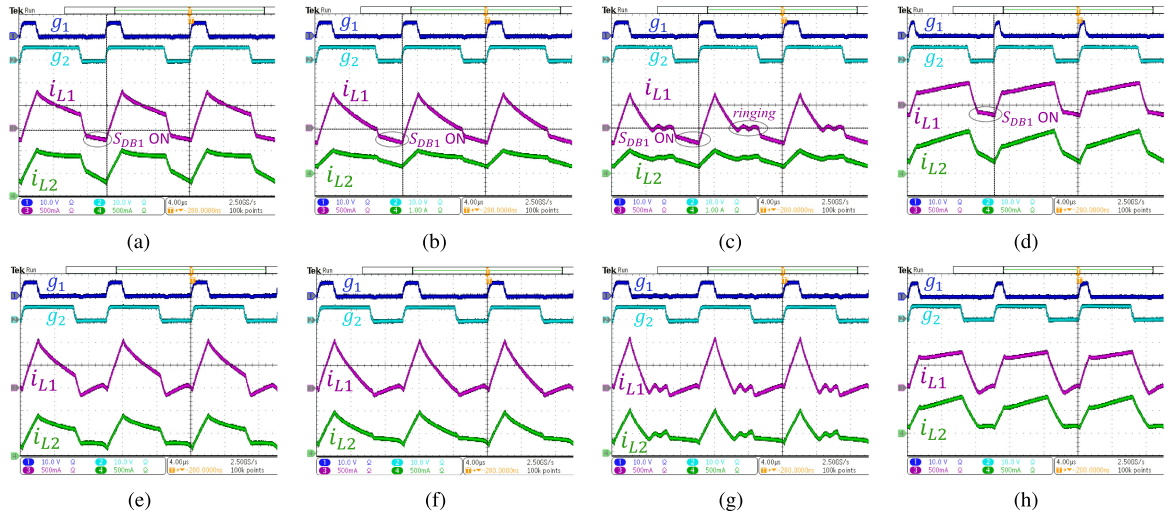

Fig. 9. Experimental results of the CI-SIDO boost converter in operating modes (a) 1a, (b) 1b, (c) 1c, (d) 3, (e) 4a, (f) 4b, (g) 4c, and (h) 6.

3) *Effect of body diode on the average values of inductor currents, diode currents, and input current:* The average value of i_{L1} may become negative when S_{DB1} is ON depending on the values of k, L_1, L_2, V_{o1}, V_{o2}, and V_{in}. As the average value of i_{in} is the sum of the average values of i_{L1} and i_{L2}, its value can take negative values depending on the average value of i_{L1} and i_{L2}. When S_{DB1} is OFF, i_{L1} is never negative. Therefore, negative i_{in} is also not possible.
4) *Effect of change in input voltage:* In practical applications where output voltages are maintained constant, the effect of variation on V_{in} is found. It is found that for a given k, L_1, L_2, V_{o1}, and V_{o2}, the range of V_{in} exists for each sector. As V_{in} increases, the converter may remain in the same sector or may change the sector. In both the cases, as V_{in} increases, average values of i_{L1} decrease.
5) *Effect of change in load current and duty ratio:* As the load current of the first boost decreases and enters DCM, the average values of the first inductor current also decrease. As the second load current is not changed, there is no significant change in the average values of the second inductor current. With the decrease in i_{o1}, D_1 decreases in DCM whereas D_2 changes with V_{in} as it is in CCM.
6) *Voltage and current stress on semiconductors:* The current stress decreases compared with the CCM operations. However, the voltage stress depends on the voltages and coupled inductor parameters.
7) *Output voltage gain:* The input–output voltage relations depend on the input voltage, both output voltages, and coupled inductor parameters.

The analysis presented in this article helps the designers with the choice of components. As the voltage gain of the converter increases many times in DCM, the voltage ratings of the output capacitors also get affected. The selection of MOSFETs and diodes also change depending on their voltage blocking capabilities and the currents carrying capabilities of the body diodes. Also, all the waveforms of the CI-SIDO boost converter that are presented in this article will help the system operator to design the controller for the CI-SIDO boost converter in DCM.

VI. Conclusion

This article analyzes the CI-SIDO boost in DCM. The CI-SIDO boost converter combines two boost converters with a common input and a coupled inductor. It is found that the DCM operation of the CI-SIDO boost turns ON the body diode of the MOSFET. The article finds that the body diode turns ON in Sectors 1, 2, and 3 when one boost is in DCM while the other in CCM. When the body diode is turned ON, the average values of inductor currents and input current may become negative depending on the output voltage, input voltage, and coupled inductor parameters. As the load current of the first boost decreases and enters DCM, the average values of the first inductor current also decrease, whereas there is no significant change in the average values of the second inductor current. For the given output voltages, as the input voltage is increased, the average values of the inductor current decrease. The simulations are done in MATLAB/Simulink to verify the effect of input voltage and load current change on the average values of inductor currents and duty ratios. Each mode is generated in experiments using a laboratory prototype of a CI-SIDO boost converter.

References

[1] Y. Liu, G. Chen, Y. Hu, L. Huang, and X. Qing, "Magnetic coupling branch based dual-input/output DC-DC converters with improved cross-regulation and soft-switching operation," *IEEE Trans. Ind. Electron.*, vol. 67, no. 9, pp. 7167–7178, Sep. 2020.
[2] M. S. A. Jafarian and H. R. Karshenas, "Current ripple reduction in single-input, multiple-output converters using phase-shift and coupled inductors," in *Proc. Iranian Conf. Elect. Eng.*, 2016, pp. 816–821.
[3] G. Zhu, B. A. McDonald, and K. Wang, "Modeling and analysis of coupled inductors in power converters," *IEEE Trans. Power Electron.*, vol. 26, no. 5, pp. 1355–1363, May 2011.
[4] S. Song, G. Chen, Y. Liu, Y. Hu, K. Ni, and Y. Wang, "A three-switch-based single-input dual-output converter with simultaneous boost buck voltage conversion," *IEEE Trans. Ind. Informat.*, vol. 16, no. 7, pp. 4468–4477, Jul. 2020.

[5] N. Elsayad, H. Moradisizkoohi, and O. Mohammed, "A new single-switch structure of a DC-DC converter with wide conversion ratio for fuel cell vehicles: Analysis and development," *IEEE Trans. Emerg. Sel. Topics Power Electron.*, vol. 8, no. 3, pp. 2785–2800, Sep. 2020.
[6] A. Kumar *et al.*, "A high voltage gain DC-DC converter with common grounding for fuel cell vehicle," *IEEE Trans. Veh. Technol.*, vol. 69, no. 8, pp. 8290–8304, Aug. 2020.
[7] Nupur and S. Nath, "Minimizing ripples of inductor currents in coupled SIDO boost converter by shift of gate pulses," *IEEE Trans. Power Electron.*, vol. 35, no. 2, pp. 1217–1226, Feb. 2020.
[8] D. Gilabert, E. Sanchis-Kilders, P. J. Martínez, E. Maset, A. Ferreres, and V. Esteve, "Design of zero ripple current coupled inductors with PWM signals in continuous conduction mode," *IEEE Trans. Ind. Electron.*, vol. 68, no. 1, pp. 304–311, Jan. 2021.
[9] D. Gilabert, E. Sanchis-Kilders, P. J. Martínez, E. Maset, A. Ferreres, and V. Esteve, "Zero ripple current with coupled inductors in continuous conduction mode under PWM signals," *IEEE Trans. Emerg. Sel. Topics Power Electron.*, vol. 8, no. 4, pp. 4260–4269, Dec. 2020.
[10] D. Gilabert-Palmer *et al.*, "Measuring coupling coefficient of windings with dissimilar turns number or tight coupling using resonance," *IEEE Trans. Power Electron.*, vol. 33, no. 11, pp. 9790–9802, Nov. 2018.
[11] H. Kosai, S. McNeal, B. Jordan, J. Scofield, B. Ray, and Z. Turgut, "Coupled inductor characterization for a high performance interleaved boost converter," *IEEE Trans. Magn.*, vol. 45, no. 10, pp. 4812–4815, Oct. 2009.
[12] B. Ray, H. Kosai, S. McNeal, B. Jordan, and J. Scofield, "A comprehensive multi-mode performance analysis of interleaved boost converters," in *Proc. IEEE Energy Convers. Congr. Expo*., 2010, pp. 3014–3021.
[13] B. C. Barry, J. G. Hayes, and M. S. Rylko, "CCM and DCM operation of the interleaved two phase boost converter with discrete and coupled inductors," *IEEE Trans. Power Electron.*, vol. 30, no. 12, pp. 6551–6567, Dec. 2015.
[14] D. Wu, G. Calderon-Lopez, and A. Forsyth, "Discontinuous conduction/current mode analysis of dual interleaved buck and boost converters with interphase transformer," *IET Power Electron.*, vol. 9, pp. 31–41, Jan. 2016.
[15] F. Yang, X. Ruan, G. Wu, and Z. Ye, "Discontinuous current mode operation of a two phase interleaved boost DC-DC converter with coupled inductor," *IEEE Trans. Power Electron.*, vol. 33, no. 1, pp. 188–198, Jan. 2018.
[16] L. Li, Q. Zhang, R. Min, K. Liu, Q. Tong, and D. Lyu, "A current reshaping strategy to reduce parasitics-induced current distortion in discontinuous conduction mode boost power factor correction converter," *IEEE Trans. Ind. Electron.*, vol. 68, no. 3, pp. 2215–2224, Mar. 2021.
[17] K. Yao, H. Xu, Q. Li, Y. Han, and K. Yun, "Detailed oscillation analysis and parameter selection principle for boost PFC converter with RC snubber operated in DCM," *IEEE Trans. Power Electron.*, vol. 34, no. 4, pp. 3348–3369, Apr. 2019.
[18] D. Kim, G. Choe, and B. Lee, "DCM analysis and inductance design method of interleaved boost converters," *IEEE Trans. Power Electron.*, vol. 28, no. 10, pp. 4700–4711, Oct. 2013.
[19] F. Yang, C. Li, Y. Cao, and K. Yao, "Two-phase interleaved boost PFC converter with coupled inductor under single-phase operation," *IEEE Trans. Power Electron.*, vol. 35, no. 1, pp. 169–184, Jan. 2020.
[20] Nupur and S. Nath, "Maximizing ripple cancellation in input current for SIDO boost converter by design of coupled inductors," *IEEE J. Emerg. Sel. Topics Ind. Electron.*, vol. 2, no. 4, pp. 409–419, Oct. 2021.

Nupur (Student Member, IEEE) received the B.Tech. degree in electrical and electronics engineering from the National Institute of Technology, Papum Pare, India, in 2014. She is currently working toward the Ph.D. degree with the Department of Electronics and Electrical Engineering, Indian Institute of Technology Guwahati, Guwahati, India.

Her current research interests include the analysis and design of multiport dc–dc converters.

Shabari Nath (Member, IEEE) received the B.E. degree in electrical engineering from Rajiv Gandhi Proudyogiki Vishwavidyalaya, Bhopal, India, in 2005, the M.Tech. degree in electrical engineering from the Indian Institute of Technology Bombay, Mumbai, India, in 2008, and the Ph.D. degree from the University of Minnesota, Minneapolis, MN, USA, in 2012.

Since 2014, she has been an Associate Professor with the Department of Electronics and Electrical Engineering, Indian Institute of Technology Guwahati, Guwahati, India. Prior to that, she was a Product Design Engineer with Cummins, Inc., Columbus, USA, for two years. Her research interests include multiport converters, solid-state transformers, power electronic converters for renewable energy systems, and smart microgrids.